4662 *Macromolecules* **2001,** *34,* 4662−4665

Miscibility and Interactions in Poly(*N*-acryloylthiomorpholine)/Poly(*p*-vinylphenol) Blends

Juzhen Yi and S. H. Goh*

Department of Chemistry, National University of Singapore, 3 Science Drive 3, Singapore 117543

A. T. S. Wee

Department of Physics, National University of Singapore, 3 Science Drive 3, Singapore 117543

Received February 1, 2001
Revised Manuscript Received April 13, 2001

Introduction

The formation of a miscible blend between two dissimilar polymers requires the presence of specific interactions. The existence of specific interactions in miscible polymer blends can be detected by spectroscopic techniques such as Fourier transform infrared spectroscopy (FTIR),[1,2] solid-state nuclear magnetic resonance spectroscopy (NMR),[3,4] and X-ray photoelectron spectroscopy (XPS).[5−9] Our recent studies have been focused on the miscibility and interactions in blends of polymers possessing multiple types of interacting sites.[10−15] These polymers such as poly(*N*-acryloyl-*N*′-methylpiperazine) (PAMP), poly(*N*-acryloyl-*N*′-phenylpiperazine) (PAPP), and poly(*N*-methyl-4-piperidyl methacrylate) (PMPMA) are capable of interacting with proton-donating polymers through two or three types of interacting sites simultaneously.

Ether oxygen-containing polymers such as poly(vinyl methyl ether) (PVME) and poly(ethylene oxide) are miscible with many other polymers. FTIR studies have shown that the miscibility of PVME blends arises from interactions involving the ether oxygen atoms.[16−21] In contrast, there are few examples of miscible blends involving thioether sulfur-containing polymers. Brostow et al.[22] reported that poly(phenylene sulfide) is miscible with poly(phenyl sulfide ether). However, the nature of intermolecular interactions in the miscible blends was not studied. We have reported that poly(methylthiomethyl methacrylate) is miscible with several styrenic copolymers.[23,24] However, we did not make spectroscopic measurements to study the involvement of the sulfur atoms in specific interactions in these miscible blends. We now report the miscibility and interactions in poly(*N*-acryloylthiomorpholine) (PATM)/poly(*p*-vinylphenol) (PVPh) blends. PATM is structurally similar to PAMP and PAPP except that the tertiary amine groups in the repeating units of PAMP and PAPP are replaced by a thioether sulfur atom. It is of interest to study whether the thioether sulfur atoms of PATM also interact with the hydroxyl groups of PVPh as the amine nitrogens of PAMP and PAPP do.[12,13]

Experimental Section

Materials. Acryloyl chloride and thiomorpholine were supplied by Aldrich Chemical Co., Inc. Triethylamine was from Fluka Co. PVPh with a reported weight-average molecular weight of 22 000 was supplied by Polysciences, Inc.

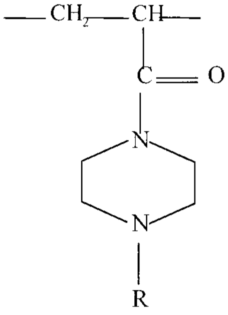

$R = CH_3$ (PAMP)

$R = C_6H_5$ (PAPP)

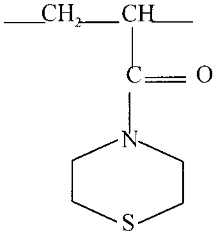

PATM

Synthesis of PATM. Thiomorpholine (0.125 mol, 12.9 mL) and triethylamine (0.175 mol, 20 mL) were dissolved in 150 mL of dry tetrahydrafuran (THF) in a 250 mL two-necked round-bottomed flask fitted with a nitrogen inlet. The flask was cooled in an ice bath (4 °C) and maintained under flowing nitrogen. THF (30 mL) solution of acryloyl chloride (0.13 mol, 10.5 mL) was added dropwise over a period of 60 min with constant stirring. The reaction mixture was then allowed to equilibrate to room temperature, and stirring was continued overnight. Triethylamine hydrochloride was removed by filtration, and it was washed repeatedly with warm THF solution. The filtrate was concentrated using a rotary evaporator. *N*-Acryloylthiomorpholine in a form of brown liquid was obtained by distillation at 102−104 °C under a reduced pressure of 5 mmHg. Hydroquinone (0.5%) was added prior to distillation to inhibit any spurious polymerization of the monomer. ^{1}H NMR: 2.27−2.64 (m, 2H + 2H, (CH_2S-), 3.83−3.93 (br, 2H + 2H, $OCN(CH_2)_2$), 5.68−5.73 (m, 1H, $CH{=}C-CON\langle$, trans), 6.24−6.30 (m, 1H, $CH{=}C-CON\langle$, cis), 6.50−6.59 (m, 1H, $={CHCON}\langle$). Elemental analysis: calculated for $C_7H_{11}ONS$: C (53.5%), H (7.0%), N (8.9%), S (20.4%). Found: C (53.2%), H (7.2%), N (8.5%), S (20.6%).

PATM was prepared by solution polymerization using azobis(isobutyronitrile) (AIBN) as initiator. *N*-Acryloylthiomorpholine (1.67 g) and AIBN (0.5 wt %) were dissolved in 50 mL of freshly distilled dioxane in a 150 mL round-bottom flask fitted with a vacuum tap. The flask was heated in an oil bath at 70 °C for 24 h with constant stirring. The viscous mixture was poured into a large volume of hexane to precipitate the polymer. The polymer was purified by two dissolution/precipitation cycles using dioxane as solvent and hexane as nonsolvent. The molecular weights (M_w = 14 000, M_n = 8000) of PATM were measured by gel permeation chromatography.

Preparation of Blends. PVPh and PATM were separately dissolved in THF to form 1% solutions. Appropriate amounts of PATM and PVPh solutions were mixed, and stirring was continued for 3 h. The solution was allowed to evaporate to dryness at room temperature. The blend was then dried in vacuo at 60 °C for 2 weeks.

GPC Measurements. The molecular weights of polymers were determined by a Waters 486 gel permeation chromatograph (GPC) with a Gordi Gel 300 mm × 4.6 mm column. The THF solutions of the polymers were first filtered through a Teflon membrane before injecting into the GPC for a 40 min run at a flow rate of 0.35 mL/min. The elution was monitored using a Waters 410 differential refraction index detector. A calibration curve was constructed using several monodisperse polystyrene standards of known molecular weights. The M_w value of the PVPh sample was found to be 20 000, which agrees well with that provided by the manufacturer.

DSC Measurements. The glass transition temperature (T_g) values of various blends were measured with a TA Instruments 2920 differential scanning calorimeter using a heating

---

* To whom correspondence should be addressed.

10.1021/ma010188m CCC: $20.00

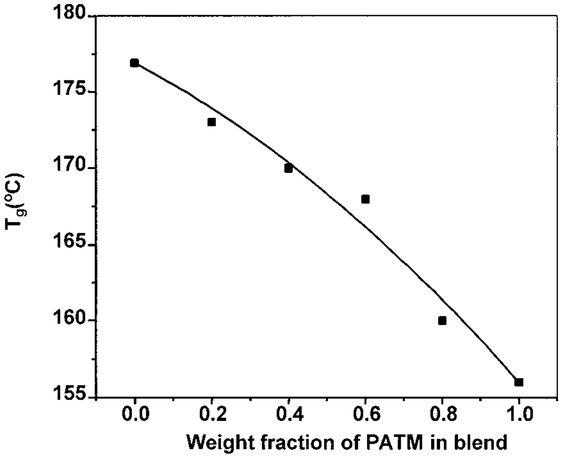

Figure 1. T_g–composition curve of PATM/PVPh blends.

rate of 20 °C/min. Each sample was subjected to several heating/cooling cycles to obtain reproducible T_g values. The initial onset of the change of slope in the DSC curve is taken to be the T_g.

FTIR Characterization. FTIR spectra were acquired using a Bio-Rad 165 FTIR spectrophotometer. All the samples were prepared by grinding the dry polymers or blends with KBr and compressing the mixtures to form disks. The disks were stored in a desiccator to avoid moisture absorption. In view of the hygroscopic nature of PVPh, all spectra were recorded at 140 °C to exclude any absorbed moisture. Sixteen scans were signal-averaged at a resolution of 4 cm^{-1}.

XPS Measurements. XPS measurements were made on a VG ESCALAB MkII spectrometer equipped with a Mg Kα X-ray source (1253.6 eV photons) and a hemispherical energy analyzer. Various blends were ground to fine powders and were then mounted on standard sample studs by means of a double-sided adhesive tape. The X-ray source was run at 12 kV and 10 mA, and a pass energy of 20 eV was used in the analyzer. The pressure in the analysis chamber was maintained at 10^{-8} mbar or lower during measurements. All core-level spectra were referenced to the saturated hydrocarbon C 1s peak at 285.0 eV.

Results and Discussion

T_g Measurements. All the PATM/PVPh blends were transparent and each showed a single T_g, indicating miscibility. As shown in Figure 1, the T_g values of the blends are slightly higher than those expected from the linear additivity rule, and the T_g–composition curve of the PATM/PVPh blends can be fitted by the Kwei equation:[25,26]

$$T_g(\text{blend}) = [(w_1T_{g1} + kw_2T_{g2})/(w_1 + kw_2)] + qw_1w_2$$

where k and q are fitting constants. The curve in Figure 1 was drawn using k and q values of 1 and 7, respectively.

FTIR Characterization. PVPh has an excellent potential for hydrogen bonding as a proton donor because of its phenolic hydroxyl groups. Figure 2 shows the IR spectra in the 3000–3800 cm^{-1} region (OH stretching) of PVPh and various PATM/PVPh blends. The hydroxyl band of pure PVPh consists of two components: a broad band centered at 3369 cm^{-1}, attributed to hydrogen-bonded hydroxyl groups (self-association), and a relative narrower band at 3525 cm^{-1}, assigned to free (nonassociated) hydroxyl groups. The center of the broad hydrogen-bonded hydroxyl band of the blend shifts from 3369 to 3384 cm^{-1}. Such a high-frequency shift indicates that the self-association of PVPh is stronger than the intermolecular hydrogen-bonding interaction between PVPh and PATM. Miscible blends of PVPh with PMPMA,[10] poly(methyl methacrylate),[27] and poly(vinyl acetate)[28] also show similar high-frequency shifts of the hydroxyl bands. As the PATM content in the blends increases, the intensity of the free hydroxyl band at 3525 cm^{-1} decreases, indicating that more free hydroxyl groups are involved in intermolecular association with PATM.

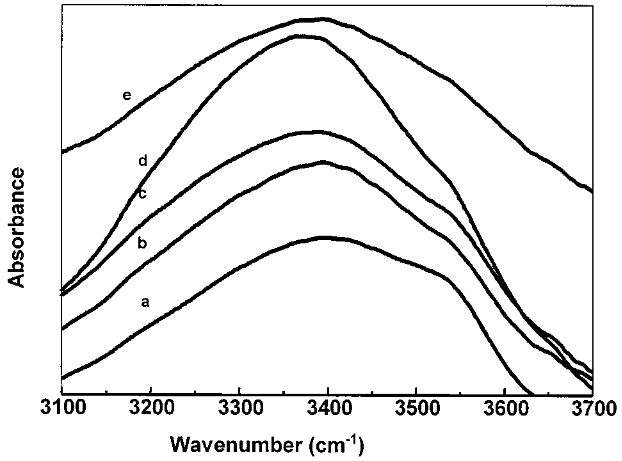

Figure 2. FTIR spectra, recorded at 140 °C, of the hydroxyl stretching region of PVPh/PATM blends containing (a) 100, (b) 80, (c) 60, (d) 40, and (e) 20 wt % PVPh.

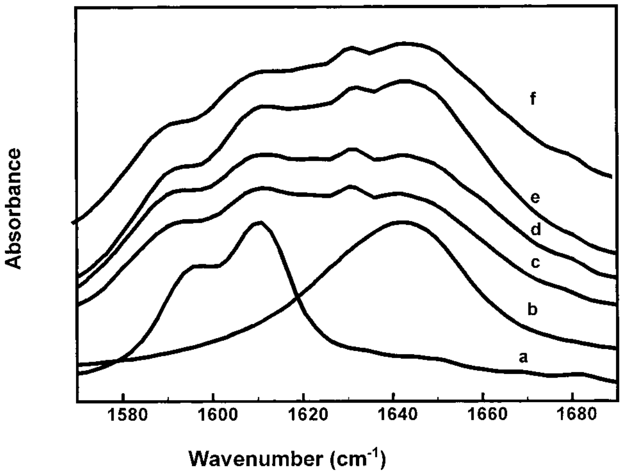

Figure 3. FTIR spectra, recorded at 140 °C, of the carbonyl stretching region of PVPh/PATM blends containing (a) 100, (b) 0, (c) 80, (d) 60, (e) 40, and (f) 20 wt % PATM.

Figure 3 shows the carbonyl stretching region of PATM/PVPh blends. The amide group of PATM may be described as a hybrid of two resonance structures with two possible hydrogen-bond interacting sites, the amide nitrogen and the carbonyl oxygen, at which interactions can occur with proton-donating polymers.[29–31] The absorption band of the amide group, the so-called amide I band, is a combination of the C=O and C–N stretching modes.[31] If the interaction is through the oxygen, the stretching energy of the C=O bond should decrease, and the infrared absorption for the carbonyl band will shift to a lower frequency. However, if the interaction is through the lone-pair electrons on the nitrogen atom, the frequency of the carbonyl band should increase.[29] Figure 3 shows the carbonyl stretching region of the FTIR spectra for PATM/PVPh blends. PATM has a strong carbonyl stretching absorption band at 1643 cm^{-1}. It is of interest to note the presence of a weak

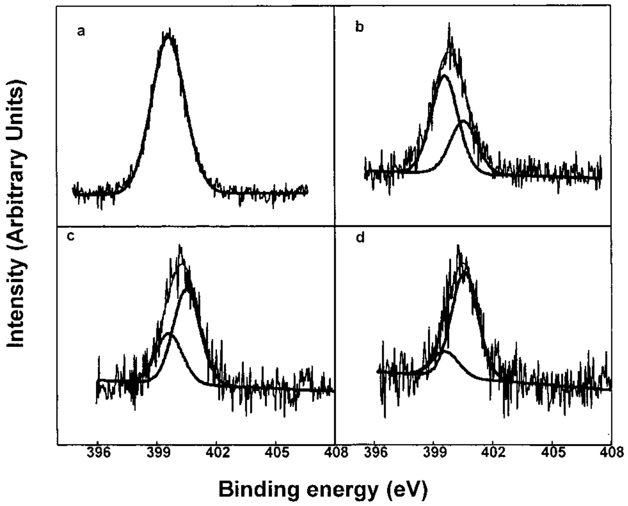

Figure 4. XPS N 1s core-level spectra of PATM (a) and PATM/PVPh blends containing (b) 20, (c) 40, and (d) 60 wt % PVPh.

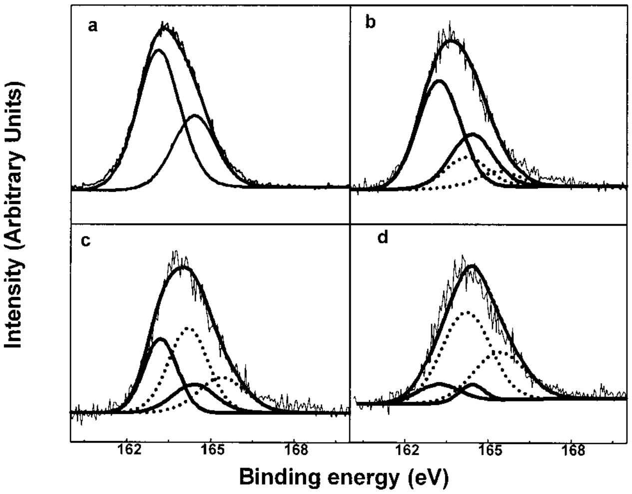

Figure 5. XPS S 2p core-level spectra of PATM (a) and PATM/PVPh blends containing (b) 20, (c) 40, and (d) 60 wt % PVPh.

shoulder band at 1653 cm^{-1} in the blends, which indicates that the hydroxyl group of PVPh interacts with the lone-pair electrons on the nitrogen atom of the amide group through hydrogen bonding. On the other hand, another new band is developed at 1633 cm^{-1}, showing the presence of hydrogen-bonding interaction between the hydroxyl groups of PVPh and carbonyl oxygen of PATM. Therefore, similar to PAMP and PAPP, both the amide nitrogen and the carbonyl oxygen of PATM interact with PVPh.

XPS Characterization. Figure 4 shows the N 1s spectra of PATM and the PATM/PVPh blends. For PATM, the amide nitrogen N 1s peak is located at 399.6 eV. The N 1s peaks of the blends are broader and asymmetric, and each peak can be deconvoluted into two component peaks, with one remaining at 399.6 eV. The presence of a new high-BE N 1s peak is evidenced in the spectra of all the blends, indicating that the nitrogen atoms in PATM interact with PVPh. The BE value of the high-BE N 1s peak is 400.6 eV. An increase of about 1.0 eV on the BE value of N 1s indicates the involvement of the nitrogen in hydrogen-bonding interaction.[5−7,10−15]

Figure 5 shows the S 2p spectra of PATM and the PATM/PVPh blends. For PATM, the S 2p spin−orbit split doublet is located at 163.2 and 164.4 eV, with an intensity ratio of 2 to 1, attributed to S $2p_{3/2}$ and S $2p_{1/2}$, respectively. The S 2p peaks of the blends are broader, indicating a change in the environment of sulfur upon blending. Each peak can be deconvoluted into two doublets, with the original doublet located at 163.2 and 164.4 eV (full curves). The peak synthesis is based on the principle that the new doublet also maintains an intensity ratio of 2:1 for S $2p_{3/2}$ and S $2p_{1/2}$, and the difference in the BE values of S $2p_{3/2}$ and S $2p_{1/2}$ is also kept at 1.2 eV. In all the cases, the sum of the intensities of the two doublets agrees well with the experimental signals. The presence of a new high-BE S 2p doublet (dashed curves) is evidenced in the spectra of all the blends, showing the interactions between the sulfur atoms in PATM and PVPh. Figure 5 also shows that the new S 2p doublet moves progressively to a high-BE region, suggesting that the interaction involving the sulfur atoms becomes more intense with increasing PVPh content. To our knowledge, this is the first report that provides a direct evidence of the involvement of thioether sulfur atoms in specific interactions in polymer blends.

Conclusions

PATM forms miscible blends with PVPh as evidenced by the transparency and the existence of a single T_g in each blend. FTIR studies show the existence of hydrogen-bonding interactions involving the carbonyl groups and the amide nitrogen atoms in PATM and the hydroxyl groups in PVPh. XPS studies demonstrate that the amide nitrogen atoms and sulfur atoms in PATM undergo hydrogen-bonding interactions with the hydroxyl groups.

References and Notes

(1) Coleman, M. M.; Painter, P. C. *Appl. Spectrosc. Rev.* **1984**, *20*, 255.
(2) Sargent, M.; Koenig, J. L. *Adv. Chem. Ser.* **1993**, *236*, 191.
(3) Guo, M. *Trends Polym. Sci.* **1996**, *4*, 238.
(4) Takegoshi, K. *Ann. Rep. NMR Spectrosc.* **1995**, *30*, 97.
(5) Goh, S. H.; Lee, S. Y.; Dai, J.; Tan, K. L. *Polymer* **1996**, *37*, 5305.
(6) Zhou, X.; Goh, S. H.; Lee, S. Y.; Tan, K. L. *Macromolecules* **1998**, *34*, 3631.
(7) Goh, S. H.; Lee, S. Y.; Zhou, X.; Tan, K. L. *Macromolecules* **1998**, *31*, 4260.
(8) Li, L.; Chan, C. M.; Weng, L. T. *Polymer* **1998**, *39*, 2355.
(9) Li, L.; Chan, C. M.; Weng, L. T.; Xiang, M. L.; Jiang, M. *Macromolecules* **1998**, *31*, 7248.
(10) Luo, X. F.; Goh, S. H.; Lee, S. Y.; Tan, K. L. *Macromolecules* **1997**, *30*, 4934.
(11) Luo, X. F.; Goh, S. H.; Lee, S. Y.; Tan, K. L. *Macromolecules* **1998**, *31*, 3251.
(12) Liu, Y.; Goh, S. H.; Lee, S. Y.; Huan, C. H. A. *Macromolecules* **1999**, *32*, 1967.
(13) Goh, S. H.; Liu, Y.; Lee, S. Y.; Huan, C. H. A. *Macromolecules* **1999**, *32*, 8595.
(14) Liu, Y.; Goh, S. H.; Lee, S. Y.; Huan, C. H. A. *J. Polym. Sci., Part B: Polym. Phys.* **2000**, *38*, 501.
(15) Huang, X. D.; Goh, S. H.; Lee, S. Y.; Huan, C. H. A. *Macromolecules* **1999**, *32*, 4327.
(16) Lu, F. J.; Benedetti, E.; Hsu, S. L. *Macromolecules* **1983**, *16*, 1525.
(17) Garcia, D. *J. Polym. Sci., Polym. Phys. Ed.* **1984**, *22*, 107.
(18) Kang, D. P.; Ha, C. S.; Cho, W. J. *J. Polym. Sci., Part A: Polym. Chem.* **1989**, *27*, 1401.
(19) Ha, C. S.; Cho, W. J.; Ryou, J. H.; Roe, R. J. *Polymer* **1993**, *34*, 505.
(20) Ryou, J. H.; Ha, C. S.; Cho, W. J. *J. Polym. Sci., Part A: Polym. Chem.* **1989**, *31*, 325.
(21) Zhuang, H.; Pearce, E. M.; Kwei, T. K. *Polymer* **1995**, *36*, 2237.

(22) Brostow, W.; Seo, K. H.; Back, J. B.; Lim, J. C. *Polym. Eng. Sci.* **1995**, *35*, 1016.
(23) Goh, S. H.; Lee, S. Y.; Chong, Y. F.; Neo, M. K.; Leong, C. L. *Macromolecules* **1991**, *24*, 806.
(24) Goh, S. H.; Lee, S. Y.; Leong, C. L. *J. Appl. Polym. Sci.* **1992**, *44*, 199.
(25) Kwei, T. K. *J. Polym. Sci., Polym. Lett. Ed.* **1984**, *22*, 307.
(26) Pennachia, J. R.; Pearce, E. M.; Kwei, T. K.; Bulkin, B. J.; Chen, J. P. *Macromolecules* **1986**, *19*, 973.
(27) Li, D.; Brisson, J. *Macromolecules* **1996**, *29*, 868.
(28) Moskala, E. J.; Howe, S. E.; Painter, P. C.; Coleman, M. M. *Macromolecules* **1984**, *17*, 1671.
(29) Feng, Y.; Schmidt, A.; Weiss, R. A. *Macromolecules* **1996**, *29*, 3909.
(30) Bull, W. E.; Madan, S. K.; Willis, J. E. *Inorg. Chem.* **1963**, *2*, 303.
(31) Lichkus, A. M.; Painter, P. C.; Coleman, M. M. *Macromolecules* **1988**, *21*, 2636.

MA010188M